

ULTRAFINE GRAIN REFINEMENT OF IRON INDUCED BY SEVERE PLASTIC DEFORMATION IN ASSISTANCE OF MULTI-DIRECTIONAL DEFORMATION MODE

Alexandra I. Yurkova^{1*}, Alexandra V. Byakova², Marina Gricenko¹

1 National Technical University of Ukraine “Kiev Polytechnic Institute”, Prospect Peremohy 37, 03056, Kiev, Ukraine

2 Institute for Problems of Material Science, National Academy of Sciences of Ukraine, Krzhyzhanivsky St. 3, 03142, Kiev, Ukraine

ABSTRACT

This study is primarily addressed to the problem of grain refinement of ferrite subjected to severe plastic deformation (SPD). In particular, ultra fine refining the original coarse grain of α -Fe was shown to be realistic using severe plastic deformation with friction (SPDF). Several structural sections of different scale regimes consisted of the grains from several nanometres at the top surface to several micrometres in the region adjacent to the strain-free matrix are formed in assistance of multi-directional deformation mode indicative of SPDF process. Structural revolution induced by SPD and governed by simultaneous high level of strain rate and temperature control was adequately described using Zener-Hollomon parameter, Z . Ultra grain refinement of ferrite down to submicrometer–nanometer scale regimes was found to be available when parameter Z exceeds the critical value roughly about 10^{16} s^{-1} . High efficiency of processes assisted by multi-directional deformation for ultra fine grain refining caused through continuous dynamic recrystallisation has been justified compared to those ensured by unidirectional deformation mode and supported by conventional dynamic recrystallisation. At the multi-directional deformation the variation of grain size d with Z parameter has a tendency to follow the equation $d = 6 \cdot 10^7 Z_0^{-0.47}$ while unidirectional deformation by shear or compression gives the equation $d = 3 \cdot 10^2 Z_0^{-0.16}$.

Key words: severe plastic deformation (SPD), iron, grain refinement, dynamic recrystallisation, Zener-Hollomon parameter

INTRODUCTION

In the recent years much attention has been paid to ultrafine grained (UFG) materials with grain sizes ranged from submicrometer- to nanometre-scale. UFG materials have been found to exhibit interesting combination of physical and mechanical properties, making them of growing interest to researches employed both in scientific and engineering applications [1-6]. However, structure and, hence, performance metrics of UFG materials are strongly

* e-mail: yurkova@list.ru ; tel: (+38)044 280 1780 tel: (+38)044 4068379

dependent on the particular route employed for their production. Compared to others routes severe plastic deformation (SPD) technique offers the essential advantages for ultra grain refining the structure of metallic materials, making them completely dense without risk of contamination. Generally, grain refinement induced by plastic deformation has been known for long time. During the last decade the efforts intent to microstructure refinement of metallic materials have been continued and tremendous progress has been achieved in material grain refining down to submicrometre- and nanometre-scale by using different techniques of severe plastic deformation (SPD) [1–6].

The formation of nanocrystalline structure with high-angle boundaries (HABs) is limited to those processes like ball milling [5, 6], surface mechanical attrition treatment (SMAT) called often by shot peening [5, 7], high speed drilling [5], hard turning [5], and sliding friction [4, 5, 8] or high-pressure torsion (HPT) [9]. Among these processes HPT is the mostly effective to produce bulk nanocrystalline materials whereas other processes are capable to give only nanocrystalline surface layers. As shown in previous papers [4, 8] high-energy friction process can result in SPD of metal, leading to generation of deformation-induced grain refinement of the surface layer and improvement properties of material work piece itself.

The present study describes characteristic features of grain refined structure created by severe plastic deformation of α -Fe pieces being subjected to friction (SPDF). Mechanism of grain refinement is discussed and clarified on the base of characteristic features of structural sections within deformation region induced by SPDF. Special attention is paid to finding the processing parameters and deformation mode responsible for ultra fine grain refinement and especially to those quite enough for creation of nanocrystalline structure.

METHODS OF SAMPLE MANUFACTURING AND ANALYSIS

Cylindrical-shaped samples of iron (purity 99.9 wt. %) with mean grain size of 80 μm with 8 mm in diameter and 50 mm in height were subjected to SPDF in argon gas using the set up described elsewhere [4, 8].

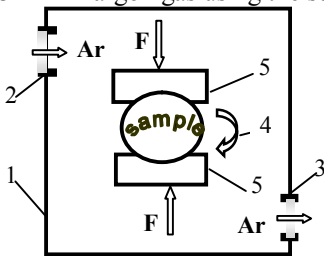


Fig. 1 – Schematic presentation of severe plastic deformation with friction (SPDF)

Fig. 1 shows schematically the set-up used for SPDF treatment. Meaningful parts of the set-up are as follow: (1) hermetically closed chamber filled by argon gas; (2), (3) system for argon gas inputting/outputting and pressure control; (4) sample rotation system; (5) two blocks of hard alloy (WC-8 % Co) being forced to the sample surface.

Sample sited between the forced blocks of hard alloy (5) was rotated with velocity about 6×10^3 rpm. Friction process

under forced blocks ensures its heating the rotated sample up to the constant temperature of 773 K. Rotation was stopped after the time about 60 min and the sample was free cooled down to the room temperature.

Structural characterisation of as-treated samples was performed on diffractometer (20 kV; 10 mA) with Fe K_{α} radiation. Stepwise X-ray diffraction (XRD) study including XRD line profile analysis was employed for estimation of the average size of coherent domains and mean dislocation density from the broadening the $(110)_{\alpha}$ and $(220)_{\alpha}$ peaks. Cross-sectional microstructure of as-treated samples was studied by using optical microscope Neophot-21. Morphology (size and shape) of refined grains and subgrains evolved by SPDF of iron samples was studied by transmission electron microscopy (TEM) images (bright and dark fields) and selected area electron diffraction (SAED) patterns performed using microscope JEM-CX (operating at a voltage of 125 kV).

RESULTS AND DISCUSSION

Fig. 2 shows cross-sectional microstructure of as-treated Fe sample observed by optical microscopy. Gradient deformation region with the overall thickness 60 μm and consisted of grains different to those of untreated α -Fe matrix is revealed in the surface layer.

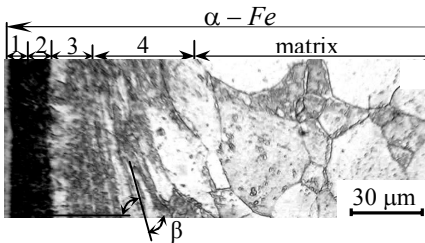


Fig. 2 – Typical cross-sectional optical observation of the as-treated Fe showing structural sections of different scale regimes

section (2) were expected to be refined down to nano- and/or submicrometre scale regimes. Section 2 is followed by section 3 consisted of fine and nearly equiaxed grains with the size ranging from 1 μm to 5 μm whereas the last section 4 adjacent to the strain-free matrix exhibits banded structure consisted of micrometre-sized (10 μm in the width) and elongated grains inclined to the sample cylindrical surface. In addition, interlayers of ultrafine and nearly equiaxed grains are sited between neighbouring pancake-shaped grains.

The results of XRD analysis show substantial broadening of Bragg diffraction peaks along the depth of deformation region compared to that for the strain-free matrix. XRD peak broadening is usually ascribed to grain refinement down to ultra fine domains as well as to increased dislocation density. According to the results of XRD line profile analysis listed in Table 1 the smallest size

Four meaningful structural sections of different grain morphology (size and shape) are well visible within deformation region, as indicated in Fig. 2. Section 1 at the top surface and adjacent to it dipper section 2 demonstrate very fine grain structure for which optical microscopy was inadequate to recognise grain size. If so, the structure of section (1) and that of

section (2) were expected to be refined down to nano- and/or submicrometre scale regimes. Section 2 is followed by section 3 consisted of fine and nearly equiaxed grains with the size ranging from 1 μm to 5 μm whereas the last section 4 adjacent to the strain-free matrix exhibits banded structure consisted of micrometre-sized (10 μm in the width) and elongated grains inclined to the sample cylindrical surface. In addition, interlayers of ultrafine and nearly equiaxed grains are sited between neighbouring pancake-shaped grains.

The results of XRD analysis show substantial broadening of Bragg diffraction peaks along the depth of deformation region compared to that for the strain-free matrix. XRD peak broadening is usually ascribed to grain refinement down to ultra fine domains as well as to increased dislocation density. According to the results of XRD line profile analysis listed in Table 1 the smallest size

of coherent domains about 13 nm is revealed in section 1. Moreover, this section is characterised by the highest dislocation density ranging from 10^{16} m/m³ to 10^{15} m/m³. As could be seen in *Table 1* the average coherent domain size increases gradually up to 150 nm in the direction from the top surface to strain-free matrix while dislocation density decreases steadily.

Table 1– Variation of structural characteristics along deformation region of as-treated α -Fe subjected to SPDF

Structural sections	Distance to surface (μm)	XRD analysis		Microscopy results
		Size of coherent domain (nm)	Dislocation density ρ (m/m ³)	Mean grain size d (nm)
1	0	13	$8.9 \cdot 10^{15}$	20*
1	3	18	$7.8 \cdot 10^{15}$	70*
2	10	23	$7.2 \cdot 10^{15}$	150*
2	20	37	$6.5 \cdot 10^{15}$	400*
3	30	70	$4.5 \cdot 10^{15}$	1000**
3	40	112	$2.5 \cdot 10^{15}$	2000**
4	50	146	$8.5 \cdot 10^{14}$	3000**
4	60	–	$5 \cdot 10^{14}$	7000**
strain free matrix		–	10^{11}	80000**

* data obtained by observation of TEM images and ** optical micrographs

Fig. 3 shows detailed cross-sectional TEM observations of the structure and corresponding SAED patterns attributed to the each of four sections created in the deformation region of as-treated Fe sample. Diffraction rings/spots in the SAED patterns attributed to all of the sections correspond to α -Fe, and no other phases were detected. In the sections numbered by 1, 2, and 3, the ringed SAED patterns with a great number of point reflections indicate the presence of ultrafine equiaxed grains with random crystallographic orientations.

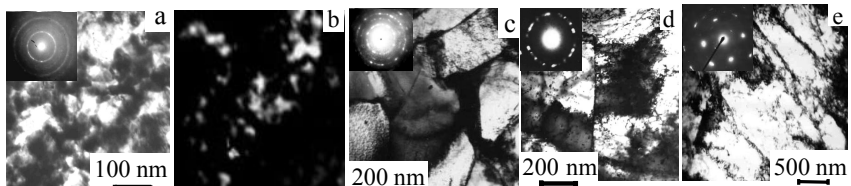


Fig. 3 – TEM images and SAED patterns of different structural sections of as-treated α -Fe: (a, b) –section 1 (of 1 μm deep to the top surface) (a) – bright-field image; (b) – dark-field image in $(110)_{\text{Fe}}$ reflection; (c) – section 2 (of 10 μm deep to the top surface); (d) – section 3 (of 30 μm deep to the top surface); (e) – section 4 (of 40 μm deep to the top surface)

Within the section 1 the number of point reflections located on the Debye rings is the greatest while their size is the smallest, indicating the presence of mostly fine grains at the top surface. Grain size measured using duck-field TEM images was believed to be about 20 nm at the top surface of section 1, as depicted in *Fig. 3b*. Correlation of TEM observation to XRD results determined for section 1 seems to be good, indicating for this case that the average size of coherently diffracting regions reflects actual grain size d , as could be seen in Table 1. If so, refined grains of actual crystal structure are formed in section 1.

As shown in *Fig. 3*, number of the point reflections presented on the debye rings of SAED patterns decreases along the depth of the sections 2 and 3 while their size increases step by step, demonstrating the increasing of grain size toward the free-strain matrix. It is noticeable that SAED pattern for section 4 consists of individual spots indicative of coarse grained Fe.

Generally, the results of plastic deformation are defined by dislocation activities in metals and depend strongly on crystal structure and stacking fault energy (SFE). For example, in materials with low SFEs, plastic deformation may only originate transformation from dislocation slipping to mechanical twinning while in materials with high SFEs and, in particular, in iron, where dislocation mobility is much higher, dislocation walls (DW) and cells will be formed, finally resulting in formation of sub-boundaries within the original grain. The refinement process of coarse grains upon plastic deformation, in principle, depends on many extrinsic factors such as intensity of strains and strain rates, deformation temperature, and so on. Apart from, dominating mechanisms and clear sceneries for ultra fine refining the coarse grains into the nanometer sized crystals are yet far from understanding.

Generally, three different mechanisms for deformation-induced grain refinement of ferrite under elevated temperatures are presently discussed in literature: (i) dynamic recovery (DRC) [10-13], (ii) conventional dynamic recrystallisation (DRX) [10-15], (iii) continuous dynamic recrystallisation (CDRX) or, equivalently, recrystallisation in situ [6, 12, 16-20]. The levels of strain and strain rate are commonly considered as basic regulative factors to initiate the ultra grain refinement by one or another mechanism.

As applied to subject matter SPDF process provides for unique opportunity to investigate the grain refinement mechanism owing to gradient variation of the strain and strain rates along the depth of deformation region. This means that microstructure features (including grain size and grain boundary misorientations) at the different sections of deformation region could be attributed to different levels of strains and strain rates. Therefore, one or another underlying mechanism for deformation-induced grain refinement in different scale regimes ranged from nanometre to micrometre levels can be recognised and specified.

The stored true strain, ϵ , along the structural sections involved in deformation region induced by SPDF process was estimated from dislocation densi-

ty, ρ , using the relation originally proposed in [6]: $\rho = 1,87 \cdot 10^{15} e^{0.6}$. In addition, following [21] stored true strain e operating the structural section 4 was derived from the shear strain, γ , being determined using the angle of grains slope, β , as shown in Fig. 2. It is noticeable that the values of true strain estimated in section 4 by two different ways were in good agreement. The results of calculations show that both extremely high stored strain about $13.5 \dots 10$ and strain rates about $10^4 - 10^3 \text{ s}^{-1}$ arise at the top surface of the sample and dropped steeply along the deformation region toward the strain free matrix.

The results show that structural sections 1, 2, and 3 consist of equiaxed grains with HABs, suggesting their formation through CDRX. The important point concerns the fact that the grain refinement in the sections above occurs under hot-to-warm working. Indeed, processing temperature about 773K was very close to the regular recrystallisation temperature, T_r . Moreover, T_r tends to decrease as the level of stored strain e increases.

Flattened shape of original grains with deformation-induced LABs formed in section 4 indicates the fact that dynamic recovery under warm working dominates structural evolution under considerable decreasing the stored strain and strain rate, as shown in Fig. 2, 3e. Development of CDRX micrometre-sized grains within interlayers between original grains is additional notable characteristic of banded structure in section 4. The former phenomenon is attributed to the large strain gradients evolved near initial grain boundaries and around triple junctions, as was pointed out in [20]. Strain incompatibilities between joint grains lead to formation of strain-induced LABs [20, 22, 23] followed by their fast transformation into HABs [24, 25]. Thus, it can be resumed that the level of stored strain and strain rate is not enough to refine completely grain structure of section 4 through CDRX.

Several aspects could be mentioned here. First of all the important point is that the transformation of cellular structure to granular one is achieved when dislocation density reached the critical density that was believed to be not less than about 10^{14} m/m^3 while the limit of dislocation density being achieved by SPD processes does not usually exceed 10^{16} m/m^3 [6]. Therefore, grain refinement continues to advance until dislocation multiplication superior to dislocation annihilation. Stabilized grain size is formed when refinement process gets the steady state at the balance between dislocation multiplication and annihilation. As pointed out in literature [7, 18] stabilised grain size is probably limited to about 10 nm since deformation takes place mainly by grain boundary sliding and/or grain rotation.

The next aspect concerns the fact that different levels of stabilized grain sizes are available by using different technical approaches. It seems that deformation mode contributes directly in final results of microstructural revolution induced by SPD. In fact, SPD techniques [4-8, 18] assisted by multi-directional

deformation are commonly considered to be mostly effective in term of their application for ultrafine grain refinement of α -Fe down to nanometre-scale level. Unlike to this grain refinement below submicrometre scale is probably difficult to achieve in processes assisted by unidirectional deformation. As evidenced from the data published in literature, application of multi-directional deformation involving compressive and shear modes is greatly beneficial in fast strain storage and generation of dislocations as compared to unidirectional deformation by shear. Nevertheless, assessment of techniques in term of their effect on grain refinement efficiency and finally stabilised grain size is rather complicated because of the differences in combination of strain rate and achievable stored strain, resulted from differences in deformation mode and temperature conditions.

The theory advanced in the latest publications [11, 14, 26] for grain refinement by repeated deformation could be viewed as that adequately describing grain formation in the regime governed by simultaneous high level of strain rate and temperature control. As applied to subject matter deformation-refined grain size has generally been reported with variation of Zener-Hollomon parameter, Z , presently considered as valuable criterion to govern a competitive effect of dislocation accumulation under high strain rate and dislocation annihilation caused by temperature. Following expression is commonly [14, 26] used for calculation of Z parameter with allowance for the effect above:

$$Z = \dot{\epsilon} \exp(Q/RT) \quad (1)$$

where $\dot{\epsilon}$ is strain rate in s^{-1} , Q is activation energy of deformation that is closed to the activation energy of volume diffusion of metallic atom (254 kJ/mol for ferrite iron); T is deformation temperature in K; $R = 8.31$ J/mol·K is universal gas constant.

According to [14, 15, 26] empirical relationship between finally stabilised grain size and Z parameter was given in convenient form:

$$d = kZ^{-m} \quad (2)$$

where d is grain size in μm ; k is numerical constant.

Following the procedure at which dependence of stabilised grain size on parameter Z is determined in logarithmic co-ordinates, the applicability of Eq. (2) in predicting final results under the present conditions was verified, as shown in *Fig. 4*. Actually, the data obtained in the present study for different structural sections are fitted well to a straight line. Moreover, the data reported in literature [6, 7, 13, 18] for grain refinement of α -Fe produced via the other processes being assisted by multi-directional deformation line up well on the strait line together with those determined in the present study.

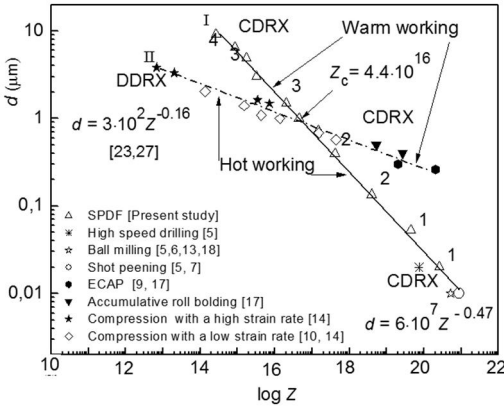


Fig. 4. Variation of grain size, d , of ferrite vs parameter Z for (I) multi-directional deformation mode, (II) unidirectional deformation mode either by shear or compression. Numbers at the strait (I) indicate structural sections in deformation region of as-treated α -Fe subjected to SPD

parameter could be expressed by the equation $d = 6 \cdot 10^7 Z^{-0.47}$ while it has a tendency to follow the expression $d = 3 \cdot 10^2 Z^{-0.16}$ under unidirectional deformation mode.

It is noticed that the value of constant and powder index at the Z parameter found under unidirectional deformation mode are numerically almost the same as those reported previously [10, 14, 26].

Several important conclusions could be derived from the data exhibited in First of all, it is clear that deformation-refined grain becomes smaller as parameter Z increases. Nevertheless, grain refinement of ferrite to submicrometer-, nanometer-scale level would be achieved when parameter Z exceeds the critical value Z_c roughly about 10^{16} . Apart from, as modified Zener-Hollomon parameter Z increases up to the value Z_c by using multi-directional deformation mode controlling effect on grain refinement is passed from CDRX under warm working to CDRX under hot working while at the unidirectional deformation mode DDRX under hot working was changed to CDRX under warm working. The next aspect concerns the fact that the value of Z parameter required for grain refinement down to nanometer-scale regime through CDRX mechanism is much smaller at the multi-directional deformation mode under hot working than that for processes supported by unidirectional deformation mode in assistance of CDRX under warm working. In particular, the value of Z parameter higher than 10^{19} is quite enough to ensure finally stabilised grains of nanometre-sized level under hot working performed by multi-directional deformation mode. Unlike the above it is easy to show that Z parameter has exceed the

However, the stabilised grain size of α -Fe achieved in processes being assisted by unidirectional deformation mode [14, 17], form different strait line with the slop that is smaller than that for the straight line joining the data determined by multi-directional deformation, as shown in Fig. 4. Thus, m power and numerical constant k in Eq. (4) are found to be variable and depend on the deformation mode. At the multi-directional deformation mode the variation of grain size d with Z para-

value about 10^{31} to achieve nanometre-sized grains of ferrite under warm working performed by unidirectional deformation mode. This means that in assistance of CDRX under warm working strain rates should be maintain at the level ranged on the order magnitude from 10^3 to 10^{13} s^{-1} that is hardly achieved by using presently developed SPD techniques performed by unidirectional deformation mode.

CONCLUSIONS

As a general conclusion it should be resumed that multi-directional deformation assisted by CDRX during straining under hot-to-warm working greatly facilitates grain refinement down to submicrometer-, nanometre-scale regimes although DDRX provided by unidirectional deformation mode during straining under hot working has a preference in grain refinement limited to the micrometre-scale regime.

The results of the present study hold the key for greater understanding the underlying mechanisms and kind of deformation mode operating ultrafine grain refinement of ferrite under severe plastic deformation and also could be promising for both the current basic research and application in engineering practice.

Acknowledgements

This work was funded by two projects: # 2211 of Ministry of Education and Science of Ukraine and NAS of Ukraine “Nano-Systems, Nano-Materials and Nano-Technologies”

REFERENCES

- [1] R. Valiev, Y. Estrin, Z. Horita, T.G. Langdon, M.J. Zehetbauer, Y.T. Zhu, The Journal of Materials 2006, Vol. 58, P. 33-39.
- [2] Nanomaterials by Severe Plastic Deformation (Eds M.J. Zehetbauer and R.Z. Valiev), Weinheim, Austria: Wiley-VCH, 2004.
- [3] Nanomaterials by Severe Plastic Deformation (Editor Z. Horita), Uetikon-Zurich, Switzerland: Trans Tech Publications, 2005.
- [4] A.I. Yurkova, A.V. Byakova, A.V. Belots'ky, Yu.V. Milman, Materials Science Forum, 2006, Vols. 503-504, P. 645-650.
- [5] M. Umemoto, Y. Todaka, J. Li and K. Tsuchiya, Materials Science Forum, 2006, Vols. 503-504, P. 11-18.
- [6] S. Takaki, Material Science Forum, 2003, Vols. 426-432, P. 215-222.
- [7] N.R. Tao, Z.N. Wang, W.P. Tong and et al., Acta Mater 2002, Vol. 50, P. 4603-4616.
- [8] Yurkova AI, Milman YuV, and Byakova AV. Russian Metallurgy (Metally), 2010, Vol. 2010, No. 4, P. 249-257.
- [9] R.Z. Valiev, Y.V. Ivanisenko, E.F. Rauch, and B. Baudelet, Acta Mater, 1996, Vol. 12, P. 4705-4712.
- [10] S.V.S. Narayana Murty, S. Torizuka, K. Nagai, and et al., Scripta Mater, 2005, Vol. 53, P. 763-768.
- [11] S.V.S. Narayana Murty, S. Torizuka, K. Nagai and et. al., Scripta Materialia, 2005,

- Vol. 52, P. 713-718.
- [12] A. A-Zadeh , B. Eghbali, *Mater Sci Eng A*, 2007, Vol. 457, P. 219-225.
- [13] Z.G. Liu , H.J. Fecht, M. Umemoto, *Mater Sci Eng A*, 2004, Vols. 375–377, P. 839-843.
- [14] J-H. Kang, S. Torizuka, *Scripta Mater*, 2007, Vol. 57, P. 1048–1051.
- [15] S.V.S. Narayana Murty, S. Torizuka, K. Nagai, *Mater Sci Forum*, 2006, Vols. 503-504, P. 687-692.
- [16] A. Belyakov, Y. Kimura, K. Tsuzaki, *Material Science and Engineering F*, 2005, Vol. 403, 249-259.
- [17] B.Q. Han, S. Yue, *J. Materials Process Technol* 2003;136:100-104.
- [18] Y. Xu, M. Umemoto, and K. Tsuchya, *Materials Transactions*, 2002, Vol. 43, P. 2205-2212.
- [19] A. Belyakov, Y. Kimura, Y. Adachi, K. Tsuzaki, *Mater Trans*, 2004, Vol. 45, P. 2812-2820.
- [20] N. Dudova , A. Belyakov , T. Sakai , R. Kaibyshev, *Acta Materialia*, 2010, Vol. 58, P. 3624-3632.
- [21] Y. Ohno, Y. Kaneko, and S. Hashimoto, *Mater Sci Forum*, 2006, Vols. 503–504, P. 727-732.
- [22] F.J. Humphreys, M. Hatherly. *Recrystallization and related annealing phenomena*. Oxford: Pergamon Press; 1996.
- [23] A.Belyakov, T.Sakai, H.Miura, *Mater Trans JIM*, 2000, Vol.41, P.476-484.
- [24] D. Kuhlmann-Wilsdorf, N. Hansen, *Scripta Metall Mater*, 1991, Vol. 25, P. 1557-1565.
- [25] B. Bay, N. Hansen, D.A. Hughes, D. Kuhlmann-Wilsdorf, *Acta Metall Mater*, 1992, Vol. 40, P. 205-214.
- [26] S. Torizuka, A. Ohmori, S.V.S. Narayana Murty, and K. Nagai, *Mater Sci Forum*, 2006, Vols. 503-504, P. 329-334.